Molecular Neurobiology (2018) 55:8522–8537
https://doi.org/10.1007/s12035-018-0988-x

The Endo-Lysosomal System of Brain Endothelial Cells Is Influenced by Astrocytes In Vitro

Andrea E. Toth[1,2] · Piotr Siupka[1,2] · Thomas J. P. Augustine[3] · Susanne T. Venø[1,2] · Louiza B. Thomsen[4,2] · Torben Moos[4,2] · Hannes T. Lohi[3] · Peder Madsen[1] · Karin Lykke-Hartmann[1,5,6] · Morten S. Nielsen[1,2]

Received: 17 January 2018 / Accepted: 5 March 2018 / Published online: 20 March 2018

Abstract

Receptor- and adsorptive-mediated transport through brain endothelial cells (BEC) of the blood-brain barrier (BBB) involves a complex array of subcellular vesicular structures, the endo-lysosomal system. It consists of several types of vesicles, such as early, recycling, and late endosomes, retromer-positive structures, and lysosomes. Since this system is important for receptor-mediated transcytosis of drugs across brain capillaries, our aim was to characterise the endo-lysosomal system in BEC with emphasis on their interactions with astrocytes. We used primary porcine BEC in monoculture and in co-culture with primary rat astrocytes. The presence of astrocytes changed the intraendothelial vesicular network and significantly impacted vesicular number, morphology, and distribution. Additionally, gene set enrichment analysis revealed that 60 genes associated with vesicular trafficking showed altered expression in co-cultured BEC. Cytosolic proteins involved in subcellular trafficking were investigated to mark transport routes, such as RAB25 for transcytosis. Strikingly, the adaptor protein called AP1-μ1B, important for basolateral sorting in epithelial cells, was not expressed in BEC. Altogether, our data pin-point unique features of BEC trafficking network, essentially mapping the endo-lysosomal system of in vitro BBB models. Consequently, our findings constitute a valuable basis for planning the optimal route across the BBB when advancing drug delivery to the brain.

Keywords Blood-brain barrier · Endo-lysosomal system · Porcine brain endothelial cells · Receptor-mediated transcytosis · Vesicular transport

Introduction

The brain endothelial cells (BEC)-based in vitro models are one of the most versatile tools in blood-brain barrier (BBB) research for testing drug penetration toward the central nervous system [1, 2] or modelling pathological conditions [3]. The in vitro models have been particularly useful in studies of subcellular trafficking of receptors and their cargos during receptor-mediated transcytosis. Both receptor- and adsorptive-mediated transcytoses involve the vesicular system [1, 4–6] and are facilitated by cytosolic adaptor proteins [7] (Fig. 1). Vesicular pathways play an important role in cell physiology by influencing features such as signalling [8, 9], polarity [10], cell junction formation, and maintenance [11]. Furthermore, in BEC, components of the endo-lysosomal system are important players in receptor-mediated transcytosis of pharmaceutical antibodies [6, 12]. However, the underlying mechanisms are poorly understood. To optimise approaches for drug delivery to the brain, it is important to characterise the vesicular transport system in BEC.

Electronic supplementary material The online version of this article (https://doi.org/10.1007/s12035-018-0988-x) contains supplementary material, which is available to authorized users.

✉ Morten S. Nielsen
mn@biomed.au.dk

[1] Department of Biomedicine, Faculty of Health, Aarhus University, Ole Worms Allé 3, 8000 Aarhus, Denmark

[2] Lundbeck Foundation, Research Initiative on Brain Barriers and Drug Delivery, Scherfigsvej 7, 2100 Copenhagen, Denmark

[3] Research Program for Molecular Neurology, Helsinki University, Haartmaninkatu 8, 00290 Helsinki, Finland

[4] Laboratory of Neurobiology, Department of Health Science and Technology, Aalborg University, Fredrik Bajers Vej 3, 9220 Aalborg, Denmark

[5] Department of Clinical Genetics, Aarhus University Hospital, Brendstrupgårdsvej 21, 8200 Aarhus, Denmark

[6] Department of Clinical Medicine, Faculty of Health, Aarhus University, Bartholins Alle 6, 8000 Aarhus, Denmark

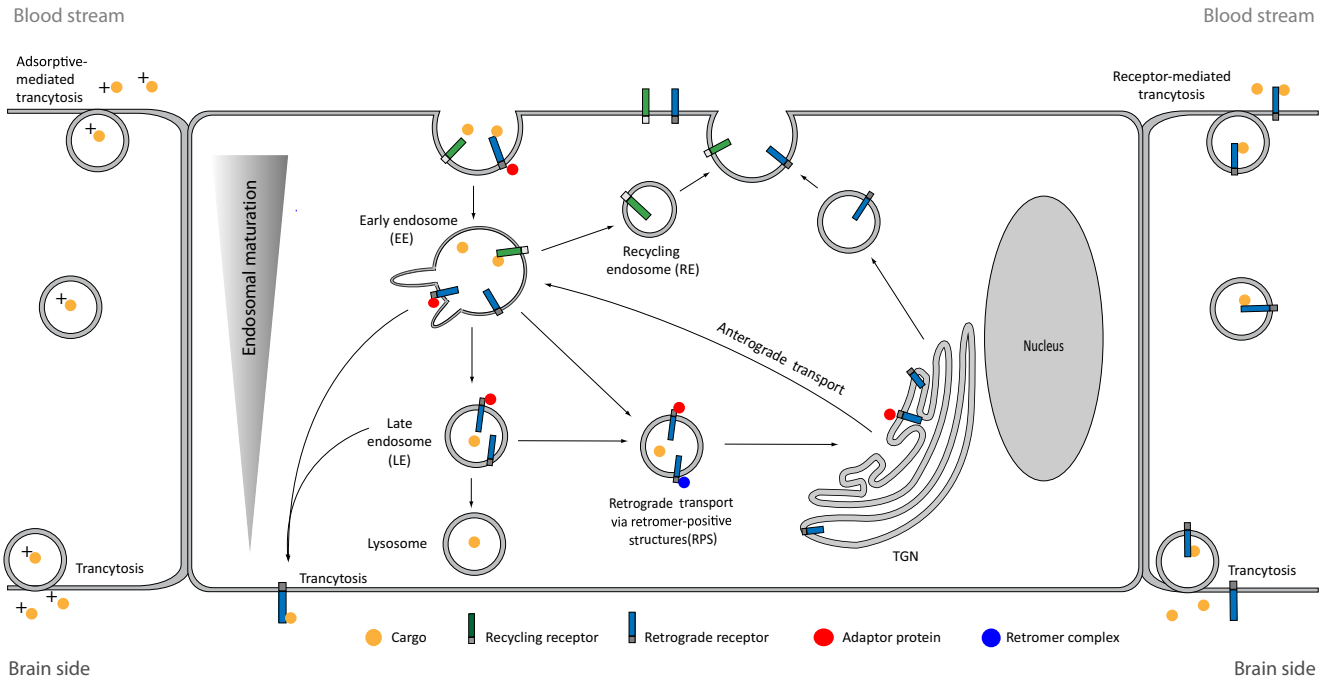

Fig. 1 Vesicular transport in brain endothelial cells. Adsorptive- and receptor-mediated transcytosis is often represented in a simple "stripped-down" way. Since the inner part of eukaryotic cells is highly compartmentalised, in reality transcytosis involves the complex endo-lysosomal system. This system consists of trans-Golgi network (TGN), several types of vesicles such as early (EE), recycling (RE), and late endosomes (LE), retromer positive structures (RPS), and lysosomes. EE are the main sorting stations in the endocytic pathway, receiving receptors and cargo from almost all types of endocytosis. The internalised membrane components and fluid are recycled back to the surface via RE, whereas retrograde receptors and certain ligands are retrograde transported to TGN via RPS. The remaining EE mature into LE and finally into lysosomes. To facilitate receptor transport, different cytosolic adaptor proteins (e.g. adaptins, retromer complex) are used by the cells

The BEC are coupled by constricting "tight junctions" and are highly polarised cells [13] similar to epithelial cells. Therefore, their drug penetration properties [14] and subcellular trafficking structures have been assumed to be similar to those of epithelial cells [7]. Transport in epithelial cells uses a complex subcellular vesicular system, the so-called endo-lysosomal system (Fig. 1). This system consists of the trans-Golgi network (TGN), several types of endosomal vesicle such as early (EE), recycling (RE), late endosomes (LE), retromer positive structures (RPS), as well as lysosomes. EE are the main sorting stations in the endocytic pathway, receiving receptors and cargo from almost all types of endocytosis [15]. The internalised membrane components and fluid are recycled back to the surface via RE [16], whereas retrograde receptors and certain ligands are retrograde transported to TGN via RPS [17]. The remaining EE mature into LE and finally into lysosomes [16]. Membrane fusion along these pathways is mediated by membrane-bound protein complexes known as soluble *N*-ethylmaleimide-sensitive factor attachment protein receptors (SNAREs) [18]. Trafficking among the structures of the endo-lysosomal system is guided by Ras-related proteins (RAB) and specific adaptor proteins such as the retromer complex [19], and the adaptins [20]. Different isoforms of the heteromeric adaptin complex can facilitate cell specific trafficking [20]. The retromer complex is composed of a conservative cargo recognition subcomplex made of the vacuolar protein sorting-associated proteins (VPS) forming a VPS26-VPS29-VPS35 trimer and a domain composed of different dimers of sorting nexins (SNX) directing the transport of the cargo [17].

To maintain and induce the specific in vivo observed BBB characteristics, in vitro cultured primary BEC need signalling factors from other cell types. One of the most important and widely studied interactions is between BEC and astrocytes. Since endothelial cells have a large repertoire of receptors for astrocyte-released agents, a range of distinct and complex responses of the endothelium has been observed [21]. Cross-talk between these cells upregulates unique BBB features in endothelial cells which results in the morphological [22] and metabolic barrier properties [23–25] and unique patterns of receptors and transporters [26] coupled with low permeability for transcellular [27, 28] and paracellular permeability markers [29] together with a high transendothelial electrical resistance [22]. To induce these specific characteristics, several methods have been developed over time [3]. One of the most commonly used techniques for primary models is to co-culture BEC with astrocytes [29] and supplement the culture media with differentiation factors such as cyclic adenosine monophosphate (cAMP) [22] and hydrocortisone [30]. In addition to having BBB-differentiating effects on BEC

themselves [31], these factors have been found to be necessary to transmit BBB-inducing effects of astrocytes by regulatory factors [32]. Given this background, we have chosen the differentiated primary porcine BEC in monoculture and in co-culture with rat astrocytes for our investigation. While the effect of astrocytes on junctional proteins and the paracellular permeability of BEC under physiological and pathological conditions has been widely studied [21, 33, 34], less is known about the transcellular permeability and vesicular transport routes across these cells.

Subcellular structures of the endo-lysosomal system in BEC (Fig. 1) are expected to play an important role in receptor-mediated transcytosis of pharmaceutical antibodies, but the brain endothelium-specific regulation of receptor trafficking and transport routes has not been investigated so far. Therefore, our aim was to investigate and characterise the endo-lysosomal system and the expressed adaptor proteins in primary porcine BEC. To obtain a better understanding of the in vivo situation, where astrocytes interact with BEC, intracellular pathways in monocultured and in co-cultured BEC with primary astrocytes were studied.

Materials and Methods

Reagents

All chemicals and reagents were purchased from Sigma-Aldrich (Rødovre, Denmark) unless otherwise indicated.

In Vitro BBB Model Constructions

Isolation of primary rat astrocytes and porcine brain microvessels was carried out as described in details in the earlier published protocol by our laboratory [35]. Briefly, cultures of glial cells were prepared from newborn Wistar rats. Meninges were removed; the cortical pieces were mechanically dissociated, plated in poly-L-lysin-coated dishes, and kept for minimum 3 weeks in DMEM containing 50-μg/ml gentamicin and 10% FBS before being frozen. Minimum of 2 weeks before co-culture, astrocytes were thawed and grown as above described in 12-well plate. Once the astrocytes reached 100% confluence, the medium was changed every 3 days. In confluent glia cultures, at least 90% of cells were immunopositive for glial fibrillary acidic protein (GFAP).

Following isolation, porcine brain capillaries were plated in T75 flasks (Thermo Fisher Scientific, Roskilde, Denmark) coated with collagen IV (500 μg/ml) and fibronectin (100 μg/ml) in DMEM/F12 medium supplemented with 10% plasma-derived bovine serum (PDS; First Link Ltd., Wolverhampton, UK), basic fibroblast growth factor (1 ng/ml), heparin (15 U), insulin-transferrin-selenium, and gentamicin (5 μg/ml) and cultured in a humidified incubator with 5% CO_2 at 37 °C. Puromycin (4 μg/ml) was added to the medium for the first 3 days to obtain a pure culture of BEC and remove contaminating cells. Cells were grown until 70% confluency then passaged onto 1.12-cm^2 polycarbonate culture inserts with 0.4-μm pore size (Costar, Corning, Kennebunk, ME, USA) at a density of 1–2 × 10^5 cells/cm^2.

Three different groups were used in this study; namely the control BEC (i), differentiated BEC (ii), and co-cultured BEC (iii) (Fig. S1a). In the control condition (i), BEC did not receive any further treatment. In the differentiated (ii) and co-cultured (iii) groups, when the BEC had reached confluence—approximately 1 or 2 days after seeding—the medium was supplemented with differentiation factors; 550-nM hydrocortisone, 250-μM 8-(4-chlorophenylthio)adenosine-3′,5′-cyclic monophosphate (cAMP), and 17.5-μM RO-201724. BEC treated with differentiation factors and grown in monoculture are referred to later as differentiated BEC (ii). In the third group (iii), BEC were kept in a non-contact co-culture with rat astrocytes on the bottom of the 12-well culture dish from the following day after seeding them on insert. When the BEC had reached confluence, approximately 2 days after co-culture, the media on BEC and astrocytes have been changed and were supplied with the above-mentioned differentiation factors daily. Sample collection was carried out 2 days after supplementing the media with differentiation factors. At this time points, the models were validated by measuring transendothelial electrical resistance. The obtained value for control (80 ± 3.5 Ω × cm^2), for differentiated monoculture (513 ± 22.91 Ω × cm^2) and for co-culture (914 ± 38.66 Ωxcm^2), was in the range of previously described data from other groups [36–38].

Antibodies

Antibodies used for immunocytochemistry and Western blot are listed in Table S1. The specificity of the antibodies for porcine BEC was confirmed by Western blot of whole cell lysates (Fig. S2). The junctions of BEC were marked with antibodies against *adherens* junction protein p120 catenin or against tight junction protein ZO1. All antibodies are commercially available and have previously been used as specific markers.

Immunofluorescence Staining and Confocal Microscopy

Cells were fixed with 4% paraformaldehyde in PBS or for RAB7 staining with methanol for 10 min at − 20 °C. Permeabilisation and blocking were done with 0.3% Triton-X100 and 1% bovine serum albumin in PBS. Primary antibodies were diluted 1:300 in blocking solution and incubated with the samples for 1 h at RT. Samples were treated with secondary antibodies at 1:400 dilutions for 1 h at RT. For

staining of the nuclei, samples were incubated with Hoechst 32528 in distilled water (0.5 μg/ml). The filters supporting the cells were cut out and mounted on glass slides using Dako fluorescence mounting medium (Dako, Glostrup, Denmark). Confocal images were captured by Olympus IX-83 fluorescent microscope with Andor confocal spinning unit and Andor iXon Ultra 897 camera, Olympus Upsalo W, ×60/1.20 NA water objective lens, using Olympus CellSens software (Olympus). Images were processed using Fiji software. For each channel, brightness and contrast adjustments were applied independently.

High Content Screening Analysis

Cells for high content screening were passaged as well onto 1.12-cm^2 polycarbonate culture inserts with 0.4-μm pore size and cultured as described above. Images were obtained with the Olympus automated Scan^R high content imaging station based on the Olympus BX73 microscope, with a ×60/0.9 NA air objective, triple-band emission filter for Hoechst 33258, Alexa-Fluor-488 and Alexa-Fluor-568, and a Hamamatsu camera (C8484-05G). Image analysis was performed using Scan^R image and data analysis software for Life Science (Münster, Germany) as described previously [39, 40]. Briefly, single-layer images were background-corrected and edge-detection algorithm was applied to segment subcellular structures based on detection of gradient intensities of the chosen colour channel. In this study, for identifying the different subcellular structures, Hoechst 33258 for nuclei, Alexa-Fluor-568 for junctions, and Alexa-Fluor-488 for vesicles were used. Subcellular structures were independently selected using the following criteria: if a closed connecting line (edge) can be drawn around them and their area is larger than 0.05 μm^2, the object is segmented. Objects are recognised and selected, independent of their shape. Images with artefacts or out of focus were manually gated out. The total number of vesicles was normalised to the number of nuclei or area of the junctions before making comparison among the adjacent groups. The distance between the objects was determined by applying Pythagoras' theorem on x, y coordinate values of the object's border. Based on the distance from the nucleus and the junctions, different zones were defined inside the cells (Fig. S1b, c, d). Above the nuclei and 1 μm around was named "perinuclear zone." Between 1 and 2 μm away from the nucleus was defined as "middle zone" of the cell. The remaining part was the processes of the cell. Since the interaction between BEC is highly important in maintaining the barrier, we investigated the junctions and 1 μm around them. In the present study, this part is defined as the "junctional zone." As endothelial cells are attached to each other all along the edges of the cells, the junctional zone overlaps partly with the other above-mentioned zones. Number, area, and morphology of vesicles from at least 1000 cells for each group and each experiment (three experiments in triplicate) were detected and analysed.

Western Blot

For Western blot, BEC were cultured in T75 flasks or co-cultured with astrocytes on 75-mm diameter polycarbonate Transwell inserts (Costar, Corning) in the above-described manner. BEC were washed with PBS and lysed in ExB lysis buffer (150-mM NaCl, 20-mM $MgCl_2$, 20-mM $CaCl_2$, 100-mM HEPES, 1% TritonX-100, cOmplete™ protease inhibitor). 2.3 μg of each protein sample was loaded on a 4–12% polyacrylamide gel (NuPage, Thermo Fisher Scientific) and subsequently transferred to nitrocellulose membrane. Before incubating with primary antibodies (1:1000) overnight at 4 °C, the membrane was blocked in 5% skimmed milk, 0.01-M Tris-HCl, 0.15-M NaCl, and 0.1% Tween 20, pH 7.6 in buffer solution. Secondary HRP-conjugated antibodies (1:2000) were applied for 1 h at room temperature. Finally, bands were detected with using ECL (GE Healthcare) or SuperSignal (Thermo scientific, Rockford, USA) according to the manufacturer's recommendations and visualised using LAS 4000 (Fujifilm). For the complete list of antibodies used in this study, see Table S1.

Next Generation Sequencing (NGS) Data Analysis

Total RNA was extracted from porcine microvascular BEC kept in monocultures and in co-cultures with astrocytes using the PicoPure RNA Isolation Kit (Arcturus Bioscience Inc., Mountain View, CA, USA). RNA was reverse transcripted to cDNA and subjected to linear amplification using the Ovation® RNA-Seq System V2 kit (NuGEN Inc., San Carlos, CA, USA). Finally, RNA-seq libraries were constructed using Illumina TruSeq DNA Sample and Preparation kit (Illumina, San Diego, CA, USA) according to the manufacturer's protocol. The integrity of libraries was validated using Agilent Bioanalyzer 2100 and library yield was determined by KAPA qPCR measurement. Sequencing was performed on an Illumina HiSeq2000 platform (Illumina) with five random samples per lane (AROS Applied Biotechnology). The raw reads reported for each sample were aligned to the ENSEMBL porcine reference using "Tophat2" [41]. The number of reads mapping to each genomic feature (i.e. genes) was determined using HTSeq (htseq-count) [42]; the count method used was "union." This measure was used as a quantitative estimate of the expression levels of features. Count-based differential expression analysis (DE) was done for the samples using DESeq2 [43]. The expression ratios are represented on the alternative transformation of logarithm base 2 [44]. Gene set enrichment analysis was performed on those genes that displayed significant (adjusted $p \leq 0.05$) differential expression using GSEA software [45] and Kyoto

Encyclopedia of Genes and Genomes (KEGG) pathway analysis [46], in order to determine underlying biological themes and pathways.

Validation of NGS Results with qPCR Analysis

Total RNA was extracted from the samples as described above. Primers were designed using an exon-spanning approach when possible using the NCBI Primer BLAST (https://www.ncbi.nlm.nih.gov/tools/primer-blast/). Selection of genes for qPCR verification was performed using the statistical algorithm NormFinder [47] to define a stability value for key reference genes based on the NGS data (Table S2). In this study, total RNA (25 ng) from each sample was used as input to an RNA amplification step using the WT-OvationTM PicoSL WTA System A (NuGEN Technologies, Inc., CA, USA) including both oligo d(T) and random hexamers for cDNA amplifications, and 100-ng cDNA was used in each SYBR green (Roche, Hvidovre, Denmark) qPCR reaction. Real-time quantitative PCR (RT-qPCR) was performed using Brilliant SYBR Green Master Mix (Roche). The PCR reactions were run in the Roche LightcyclerR96 (Roche) with the following protocol: 10-min DNA polymerase activation at 95 °C, 45 cycles of 10-s denaturation at 95 °C, 10-s annealing at 60–66 °C (gene specific), and extension at 72 °C for 10 s, followed by a final denaturation step until 95 °C over 5 min. Experiments were repeated at least three times, each in three technical repeats. The expression value of each gene relative to the reference gene (*ACTB*) was calculated using ΔΔCT methods [48]. As a negative control, cDNA from no template RT-qPCR reactions was used. For each primer pair (Table S2), a dilution curve was generated and only primer pairs with efficiency of 80–100% were included.

Statistical Analysis

All data presented are means ± SEM. Values were compared using one-way ANOVA followed by Tukey's multiple comparison post hoc tests using GraphPad Prism 6.0 software (GraphPad Software Inc., San Diego, CA, USA). Where only two variables were compared, unpaired *t* test with Welch's correction analysis was applied. Statistical analysis for NGS analysis is described above. Changes were considered statistically significant at $p \leq 0.05$. All experiments were repeated at least three times; the number of parallel samples for each experiment was at least three.

Results

To classify and quantify the different types of vesicles (Fig. 1), early endosome antigen 1 (EEA1) was targeted as a specific marker for EE [49], transferrin receptor (TfR) for RE [50], Ras-related protein 7 (RAB7) for LE [51], lysosomal-associated membrane protein 1 (LAMP1) for lysosomes [52], and VPS35 for the RPS [19] (Fig. 2). These markers are all standard markers for the given vesicular structures but do not necessarily have functions in vesicular receptor trafficking, like TfR and Lamp1.

Number of Vesicles

By applying the above-mentioned vesicle markers and analysing the result by high content screening microscopy, we were able to investigate the number of different types of vesicle. Data from differentiated and co-cultured BEC were normalised to the control (Fig. 3). Co-cultured BEC displayed upregulation in the numbers of EE and RPS and downregulation in the RE and LE. Changes in the differentiated BEC showed the same trend as observed in the co-cultured group but were significant only in the case of RPS compared to the control. The influence of astrocytes was investigated by comparing the differentiated BEC to the co-cultured group. Significant differences in the numbers of EE, RE, and LE were found. Interestingly, the number of lysosomes was not influenced significantly in any of the groups.

In order to see which part of the BEC is particularly affected by the changes, we investigated the number of vesicles in different zones of the cells (Table 1) related to their position from the nucleus and the junctions (Fig. S1b) and normalised to the control. The size of the nuclei (area 106.61 ± 0.3 μm^2; diameter 11.65 ± 0.5 μm) and the outlined junctional area (147 ± 0.07 μm^2) did not vary significantly among the different groups. An elevated number of EE could be observed in all zones of the cell, however, only significantly in the middle zone and in the processes. The increase observed in co-culture reached almost 30% in the middle zone and more than 50% in the processes (Table 1). Decrease in RE was generally observed in all zones of co-cultured cells to about the same extent as in Fig. 3 (Table 1). The most dramatic change could be seen in the processes and in the junctional zone. The number of LE dropped significantly in all zones of the cells but predominantly near the junctions (Table 1). The increase in RPS peaked in the processes in both groups. Although the total number of lysosomes did not change substantially (Fig. 3), we could see a significant peak in the processes of co-cultured BEC (Table 1). These results indicate that astrocytes do not affect the total number of lysosomes but may influence their number in different subcellular zones, i.e. redistribute them inside BEC.

Subcellular Distribution of the Vesicles

Subcellular redistribution of the vesicles even without affecting their total number inside the cells may indicate altered

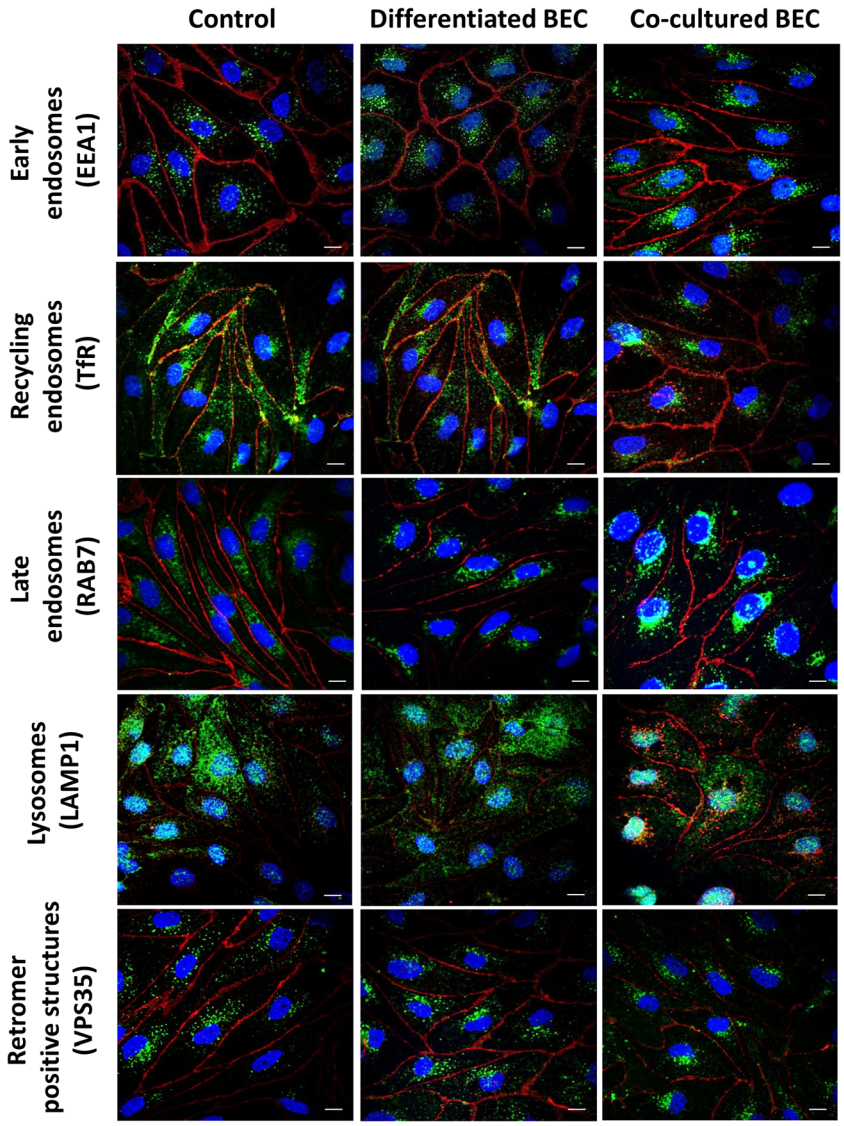

Fig. 2 Immunofluorescence staining against endosomal markers in control, differentiated, and in co-cultured BEC in vitro. Immunostaining for vesicles is represented with green and for cell border marker p120 catenin with red. Nucleus is marked with blue (Hoechst 33342). Specific markers: for early endosomes EEA1 (early endosome antigen 1), for recycling endosomes TfR (transferrin receptor) for late endosomes RAB7 (Ras-related protein 7), for lysosomes LAMP1 (lysosomal-associated marker protein 1), and for the retromer positive structures VPS35 (vacuolar protein sorting-associated protein 35) are indicated with green on the images. Magnification is ×60. Scale bar: 10 μm

physiological function [53]. Therefore, the proportion of specific vesicle types in the subcellular zones was calculated relative to their own total number/cell (100%) and then compared among the groups (Fig. 4). Generally, about 20–25% of the EE, RE, lysosomes, and RPS were located near the nucleus, more than 35% in the middle zone and the rest (~ 40%) in the processes (Fig. 4a, b, d, e). By contrast, the distribution of LE was the reverse (Fig. 4c); the majority of the vesicles were located near the nucleus (~ 35%) and the middle zone (~ 40%), with the lowest amount in the processes of BEC. Generally, about one third of the vesicles could be found in the junctional zone (Fig. 4f). The highest number of vesicles near the junctions was observed for RE and RPS in all groups.

Examining the distributional differences among the groups, treatment with differentiation factors and co-culture with astrocytes affected the distribution of all types of vesicles (Fig. 4), with the exception of RE (Fig. 4b). We could see a shift in distribution of EE toward the processes in co-cultured BEC. Distribution of EE proved to be significantly different compared also to the differentiated BEC (Fig. 4a). A similar trend was observed for lysosomes and RPS; redistribution was significant compared to the control, but not between differentiated and co-culture group (Fig. 4d, e). On the contrary to the other type of vesicles, LE moved from the middle toward the nucleus of the differentiated and co-cultured BEC (Fig. 4c) and their number in the junctional zone of co-cultured BEC decreased significantly compared to the control (Fig. 4f).

Morphological Alteration of the Vesicles: Shape and Area

Since not only the amount of vesicles but also their size and shape can vary greatly [11, 54], we investigated their area and circularity factor (CF) in different zones of the BEC (Fig. 5).

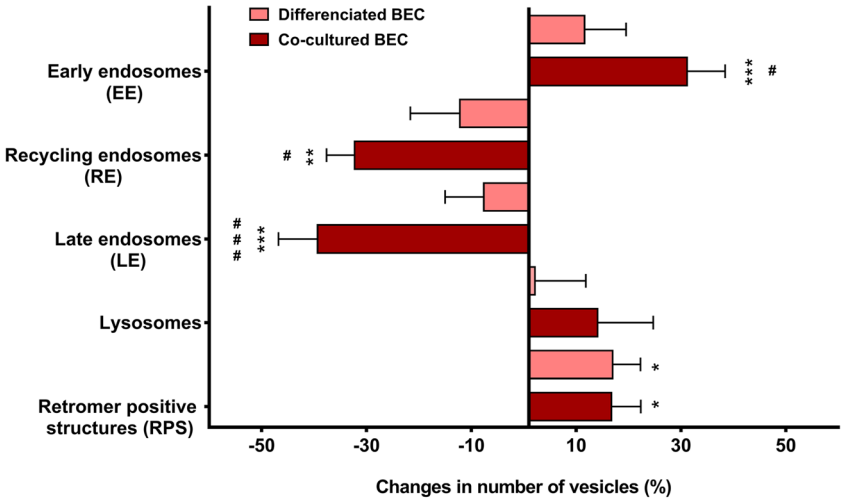

Fig. 3 Change in the number of vesicular structures normalised to control (100%). Values are represented as mean ± SEM, $n = 9$. Statistical analysis; difference was analysed by one-way ANOVA followed by Tukey's post hoc test. Values were considered statistically significant at * $p \leq 0.05$, ** $p \leq 0.01$, *** $p \leq 0.001$ compared to the control and at # $p \leq 0.05$ ## $p \leq 0.01$, ### $p \leq 0.001$ between the differentiated and co-cultured BEC. ns; not significant

Number of vesicles per cell									
	Change (%) compared to the control						Change (%) compared to the differentiated BEC		
	Differentiated BEC			Co-cultured BEC					
	Mean	SEM	*p*	Mean	SEM	*p*	Mean	SEM	*p*
EE	11.62	7.91	ns	31.15	7.29	***	17.09	6.16	#
RE	-12.19	9.44	ns	-32.26	5.36	**	-22.81	10.03	#
LE	-7.61	7.38	ns	-35.99	7.52	***	-28.39	6.78	###
Lysosomes	2.15	9.70	ns	14.11	10.62	ns	11.96	10.62	ns
RPS	10.00	2.60	*	16.67	2.60	*	6.67	2.60	ns

The shape of the investigated vesicles (CF = 1.05–1.2) was generally irregular compared to a perfect circular shape (CF = 1.00).

As shown above, co-culture with astrocytes causes similar changes in the number of EE and RPS (Fig. 3, Table 1). Consistently, we find that astrocyte-induced changes in shape and area of EE and RPS were similar (Fig. 5a, b, i, j). A pronounced effect of astrocytes on CF was observed in the processes of co-cultured BEC, while only minor changes were seen in the remaining zones of the cells (Fig. 5a, i). On the other hand, the area of these vesicles was reduced significantly near the junctions, while being close to constant in the other parts of the cells (Fig. 5b, j). For the RE, treatment of BEC with differentiation factors and the presence of astrocytes affected the shape and the size of the vesicles in all zones of the cells (Fig. 5c, d). The CF and the vesicular area were reduced significantly compared to the control, but there was no significant difference between the differentiated and the co-cultured BEC. LE did not show remarkable variation in shape or area among the groups (Fig. 5e, f). Generally, the area of LE showed a tendency of decrease, as they were located further away from the nucleus (Fig. 5f). By contrast, the shape of lysosomes became even more irregular in the differentiated and co-cultured BEC compared to the control (Fig. 5g). Lysosomes also displayed the largest variation in size among all types of vesicle (Fig. 5h).

Expression of Specific Trafficking Route-Related Genes and Proteins

Based on the observed changes in vesicular features, including size, shape, and subcellular distribution, we wanted to address potential underlying changes in gene and protein expression (Fig. 6a–c). We therefore determined the expression profiles of trafficking-related genes in BEC after co-culturing them with astrocytes (Table S3 and Fig. S3). Gene set enrichment analysis showed that 22 genes encoding lysosomal proteins and nine genes of membrane fusion mediating SNARE complexes had altered expression in co-cultured BEC (Table S4). Furthermore, distinctive expression of 29 genes involved in endocytosis and endosomal maturation had a significant impact on the endosomal part of vesicular transport. In order to show functional relevance of changes in the endo-lysosomal structure, we investigated the protein ratio of phosphorylated ERK1/2 (pERK1/2) and ERK1/2 (Fig. 6c). We found that pERK was significantly downregulated in co-cultured BEC in accordance with the altered number of late endosomes (Fig. 2). Additionally, the gene set enrichment analysis has

Table 1 Subcellular changes in the amount of vesicles. Number of vesicles was normalised to control (100%). All values are expressed as mean ± SEM, $n = 12$. Differences were analysed by one-way ANOVA followed by Tukey's post hoc test. Values were considered statistically significant at * $p \leq 0.05$, ** $p \leq 0.01$, *** $p \leq 0.001$ compared to the control. ns; not significant

Number of vesicles per cell—compared to control (%)							
		Differentiated BEC			Co-cultured BEC		
		Mean	SEM	*p*	Mean	SEM	*p*
Early endosomes (EE)	Perinuclear zone	1.11	8.91	ns	5.23	8.45	ns
	Middle zone	10.21	10.90	ns	28.55	9.57	*
	Processes zone	28.49	17.11	ns	53.32	17.11	*
	Junctional zone	1.87	20.76	ns	19.52	19.70	ns
Recycling endosomes (RE)	Perinuclear zone	− 9.65	7.86	ns	− 29.90	7.03	**
	Middle zone	4.61	9.96	ns	− 20.48	9.66	ns
	Processes zone	− 23.21	9.66	ns	− 37.02	8.14	***
	Junctional zone	− 26.74	9.30	*	− 44.91	8.70	**
Late endosomes (LE)	Perinuclear zone	− 2.89	3.82	ns	− 25.59	3.87	***
	Middle zone	− 5.88	5.57	ns	− 44.38	5.47	***
	Processes zone	− 6.65	11.67	ns	−43.98	11.67	**
	Junctional zone	− 23.04	8.62	*	−58.94	8.37	***
Lysosomes	Perinuclear zone	− 10.05	9.87	ns	3.31	11.58	ns
	Middle zone	6.77	8.93	ns	9.94	9.84	ns
	Processes zone	13.72	7.26	ns	30.19	9.10	**
	Junctional zone	− 13.50	14.20	ns	− 15.48	13.58	ns
Retromer positive structures (RPS)	Perinuclear zone	3.83	1.15	ns	1.53	2.76	ns
	Middle zone	8.62	1.31	ns	7.14	2.26	ns
	Processes zone	30.60	5.82	*	32.75	4.74	*
	Junctional zone	2.82	3.26	ns	− 0.31	3.42	ns

indicated that the MAPK pathway is significantly altered is co-cultured BEC (Table S4).

In order to investigate these changes in detail, we focused here on selected genes of cytosolic adaptor proteins essential for specific transport routes. Adaptors for retrograde transport include the heteropentameric retromer complexes [19]. We found the mRNA level of the retromer subunits in BEC were influenced by astrocytes (Fig. 6a and Table S3). Focusing on the variable SNX-BAR subunits, we observed significant changes in the *SNX1*, *SNX2*, *SNX5*, and *SNX6* genes (Fig. 6a). As retromer complexes can be regulated post-transcriptionally, we examined the protein level of SNX1 and SNX6 (Figs. 6b and S4), representing one of the two most common paring options in the SNX-BAR complex (SNX1/2 and SNX5/6) [55]. SNX1 could be detected only in co-cultured samples at a low level (Fig. 6b). Interestingly, the protein level of SNX6 (Fig. 6b) and the number of SNX6-positive structures (Fig. 6d, e) decreased prominently in differentiated and co-cultured BEC, while the total number of RPS marked by the non-exchangeable core protein VPS35 was significantly increased (Figs. 3 and 6e).

In the NGS data set, moderate downregulation of expression of the transcytotic vesicular marker *RAB25* could be observed (Table S3). However, at protein level, we did not detect any clear difference among the groups (Figs. 6b and S4).

Among the average copy number of adaptin gene transcript (AP average), *AP2* was expressed at the highest level, followed by *AP1*, *AP3*, *AP5*, and *AP4* (Fig. S3). The expression ratio of transcripts encoding the *AP1–4* subunits in co-cultured BEC was similar to the level previously described in HeLa cell line [56]. AP1 and AP3 have cell-specific μ subunits (*AP1M2* and *AP3M2*) [57]. We performed NGS and RT-qPCR analysis for these specific mRNAs. The epithelial-specific, basolateral sorting-related *AP1M2* was not expressed, but the previously known as neuron-specific *AP3M2* was present in BEC (Fig. 6a and Table S3). The specificity of *AP1M2* PCR primer was confirmed on porcine kidney epithelial tissue (Fig. 6a).

Discussion

Our study describes and classifies the endo-lysosomal system in BEC using a set of standard vesicular markers and investigates expression of selected trafficking-related genes and proteins known to be involved in endocytosis, polarised sorting, and transcytosis. Characterisation of the transport system in BEC is important for better understanding of the cellular mechanisms and trafficking routes used by receptor- or adsorptive-mediated drug delivery. We focused particularly

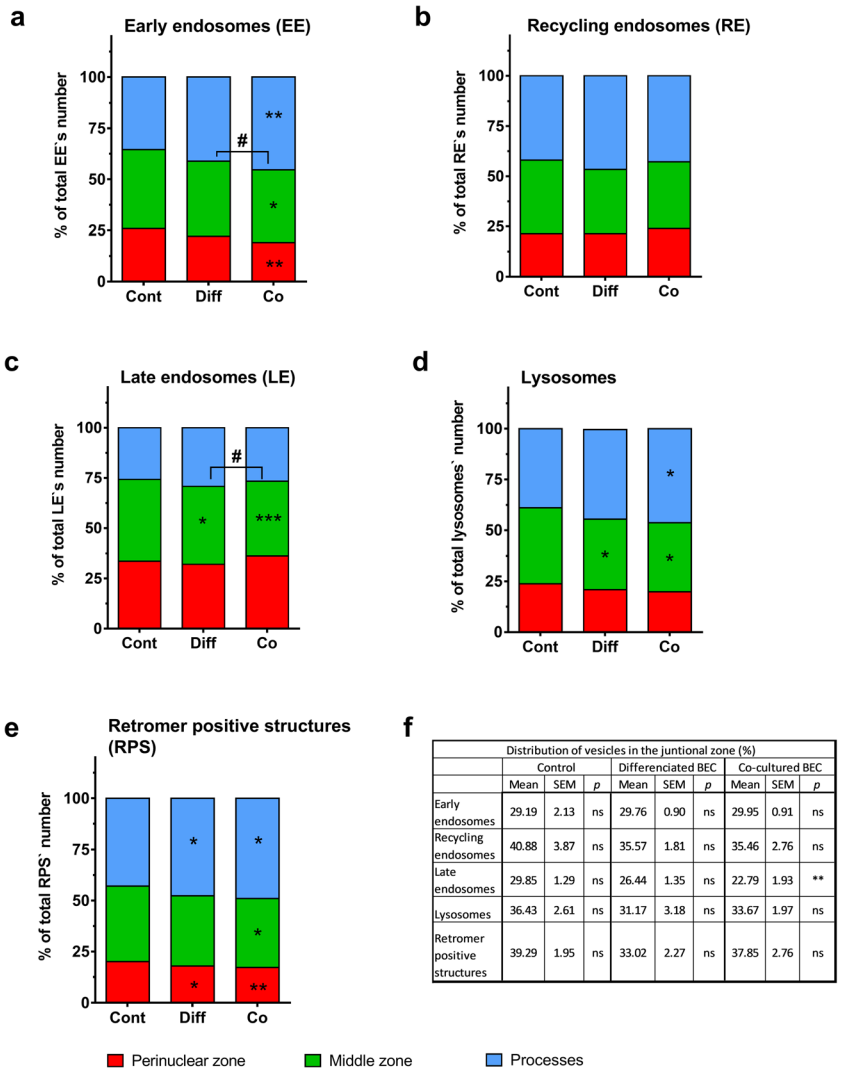

f

Distribution of vesicles in the juntional zone (%)									
	Control			Differenciated BEC			Co-cultured BEC		
	Mean	SEM	p	Mean	SEM	p	Mean	SEM	p
Early endosomes	29.19	2.13	ns	29.76	0.90	ns	29.95	0.91	ns
Recycling endosomes	40.88	3.87	ns	35.57	1.81	ns	35.46	2.76	ns
Late endosomes	29.85	1.29	ns	26.44	1.35	ns	22.79	1.93	**
Lysosomes	36.43	2.61	ns	31.17	3.18	ns	33.67	1.97	ns
Retromer positive structures	39.29	1.95	ns	33.02	2.27	ns	37.85	2.76	ns

Fig. 4 Subcellular distribution of vesicular structures. Subcellular values are expressed as a percentage of the total intracellular vesicles for each types and presented as mean, $n = 9$. Statistical analysis; difference was analysed by one-way ANOVA followed by Tukey's post hoc test. Values were considered statistically significant at * $p \leq 0.05$, ** $p \leq 0.01$, *** $p \leq 0.001$ compared to the control (Cont) and at # $p \leq 0.05$ between the differentiated (Diff) and co-cultured BEC (Co). ns; not significant

on interactions between BEC and astrocytes, since co-cultured BEC maintain the differentiated phenotype of receptors and transcytosis more closely resembling the in vivo condition [58, 59]. Our findings confirm and extend previous studies on involvement of astroglia in vesicular trafficking of BEC, where astrocytes are reported to lower transcellular permeability of the BBB by 70% as confirmed in vitro [27] as well as also in vivo [28]. However, hypoxic astrocytes increase pinocytotic vesicle production of BEC [60]. Interestingly, BEC-derived extracellular vesicles can be taken up by astrocytes [61]. In our co-culture model, we found that astrocytes affected genes involved in endocytosis, endosomal maturation, and membrane fusion-related gene expressions (Table S4) elevated the number of EE and RPS, while both RE and LE declined to the same extent (Fig. 3). These data suggest that astrocytes influence the endosomal maturation process and vesicular trafficking of BEC. Our work did not aim to give absolute numbers of vesicles or trafficking-related proteins; rather, we highlighted their fold changes. We focused on horizontal differences inside the cells in vitro, because trafficking events are highly influenced by the position of TGN near the nucleus [11]. Furthermore, BEC fulfil their physical barrier function by having tight intercellular junctions [62]. Therefore, it is also important to investigate trafficking events near the junctions. Our study has provided a horizontal map of the endo-lysosomal system in BEC, which can serve as a basis for a better understanding of intracellular trafficking in BEC.

In addition to the number, we investigated the shape, area, and distribution of vesicles in BEC. Unlike in other cell types [11], we observed the shape of these vesicles to be irregular rather than round (Fig. 5). This may be partly due to the fact that BEC are flat, elongated cells [14]. EE receive cargo from all types of endocytosis and therefore they are localised mainly in the peripheral cytoplasm [63], as observed also in our BEC (Fig. 4a). By increasing the number of EE (Fig. 3), even more endosomes gathered in the processes of co-cultured BEC. In addition to EE, RE has an important sorting function in polarised cells by delivering membrane components to the

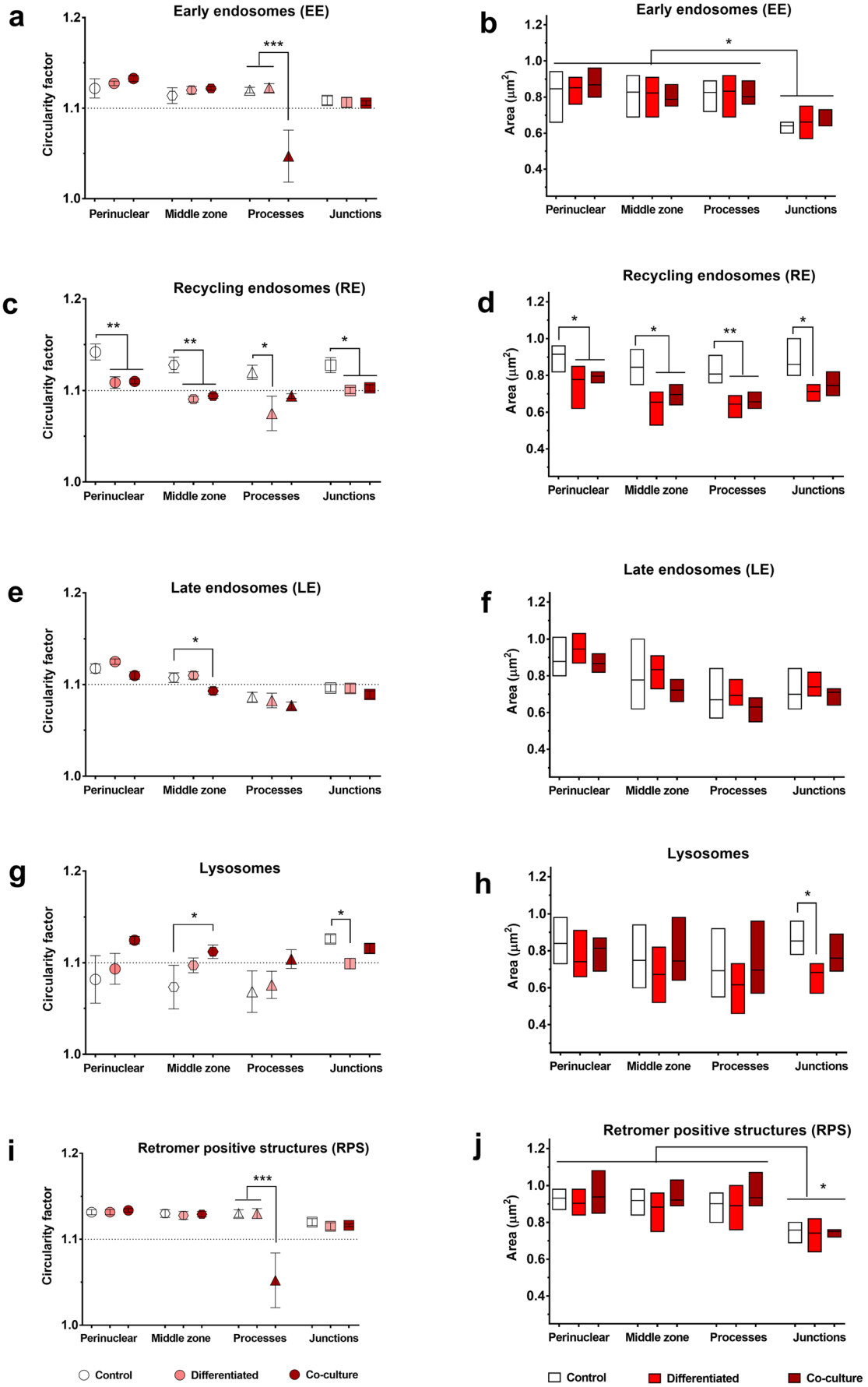
a
Early endosomes (EE)
Circularity factor
1.2
1.1
1.0
***
Perinuclear
Middle zone
Processes
Junctions
b
Early endosomes (EE)
Area (µm²)
1.2
1.0
0.8
0.6
0.4
*
Perinuclear
Middle zone
Processes
Junctions
c
Recycling endosomes (RE)
Circularity factor
**
**
*
*
Perinuclear
Middle zone
Processes
Junctions
d
Recycling endosomes (RE)
Area (µm²)
*
*
**
*
Perinuclear
Middle zone
Processes
Junctions
e
Late endosomes (LE)
Circularity factor
*
Perinuclear
Middle zone
Processes
Junctions
f
Late endosomes (LE)
Area (µm²)
Perinuclear
Middle zone
Processes
Junctions
g
Lysosomes
Circularity factor
*
*
Perinuclear
Middle zone
Processes
Junctions
h
Lysosomes
Area (µm²)
*
Perinuclear
Middle zone
Processes
Junctions
i
Retromer positive structures (RPS)
Circularity factor
***
Perinuclear
Middle zone
Processes
Junctions
Control
Differentiated
Co-culture
j
Retromer positive structures (RPS)
Area (µm²)
*
Perinuclear
Middle zone
Processes
Junctions
Control
Differentiated
Co-culture

◀ **Fig. 5** Morphological alterations of the vesicles: shape and area. The circularity factor (left panel) describes the shape of adjacent vesicles. Values are represented as mean ± SEM, $n = 9$. The area of the vesicles is shown with a box diagram (right panel); box represents 25 and 75 percentiles. The horizontal line represents the median, $n = 9$. Statistical analysis; difference was analysed by one-way ANOVA followed by Tukey's post hoc test. Values were considered statistically significant at * $p \leq 0.05$, ** $p \leq 0.01$, *** $p \leq 0.001$

appropriate place via separate transport routes. Consequently, RE can be considered as polarised vesicles with different shapes and adaptor protein composition [64]. The number, shape, and size of RE in BEC were strongly affected by astrocytes and differentiation factors (Figs. 1 and 4 and Table 1), indicating that polarity induction in BEC happens also at the level of RE. Unlike other endosomes, LE were located dominantly in the perinuclear zone (Fig. 4c), where they are able to fuse with each other as well as with lysosomes [65]. However, the number of LE decreased in co-cultured BEC (Fig. 3), with fewer lysosomes located near the nucleus and more in resting state in the processes of these cells (Fig. 4d). Interestingly, astrocytes did not affect the number of lysosomes in BEC (Fig. 3), but astrocytes did affect BEC's gene expression important for transport and synthesis of lysosomal enzymes (Table S4). Since the endosomes and lysosomes are responsible for regulation and fine-tuning of numerous pathways in the cell [8, 9], the idea that astrocytes induce some BBB endosomal properties by altering the endothelial endo-lysosomal system appears likely.

Furthermore, endosomes are also signalling platforms to ensure correct signal decoding in pathways like the mitogen-activated protein kinases (MAPK/ERK) pathways [9, 66]. This pathway is involved in transcytosis regulation in BEC [67] as well as astrocytes [27, 28]. In this signalling pathway, mitogen-activated protein kinase 1 (MEK1) promotes the activation and phosphorylation of ERK1 and ERK2 kinases [68], which is localises to the late endosomal membrane [68, 69]. We found that the level of phosphorylated ERK1/2 was significantly down-regulated (Fig. 6c) in co-cultured BEC along with the decreased number of late endosomes (Fig. 3). Based on these observations, we speculate that astrocytes might modulate these signalling pathways also via the endo-lysosomal system to induce and maintain BBB properties of BEC. Further experiments are needed to reveal the exact functional changes in BEC resulting from the signalling pathway modulating action of vesicles. In summary, we have shown that astrocytes affected not only the number of endothelial vesicles but also influenced their shape, area, distribution, and the endo-lysosomal system-related gene expression specifically.

To further investigate trafficking-related differences induced by astrocytes, we examined gene expression of BEC to pinpoint alteration with potential implication on the change in vesicular features. For transcytosis, RE are guided by RAB25 from the apical to the basolateral membrane in polarised epithelial cells [70, 71]. In our study, astrocytes moderately decreased the gene expression (Table S3) of this adaptor protein. At protein level, we confirmed the presence of RAB25 in BEC, but we could not detect significant differences among the groups (Fig. 6b). Fine-tuning of RAB25 is necessary for proper transcytosis. Silencing of *RAB25* gene inhibits transcellular transport in both directions [70], but overexpression of its protein also decreases transcytosis from the apical membrane [71]. We suggest that RAB25 can also be an important regulator of transcytosis in BEC. Further experiments needed to confirm its precise role and regulation in these cells. In the transcytotic machinery of polarised epithelial cells, the retromer, another important adaptor protein complex, is involved [72]. This complex is essential for the retrograde transport route from EE and LE toward TGN [19]. In our experiments, the number of RPS increased in differentiated as well as in co-cultured BEC (Fig. 3). The enrichment of RPS, particularly in the processes (Table 1), can be involved in lateral tubular trafficking at overlapping parts, as suggested by EM studies [73]. To study RPS, we labelled VPS35 the non-variable component of the retromer complex [19]. However, the mammalian retromer shows variability in composition of SNX-BAR dimer and VPS26 [17]. Therefore, we investigated gene and protein expression profile of the subunits of these retromers (Fig. 6a and b). At gene expression level, the most prominent differences were observed in SNX1 and SNX6 (Fig. 6a and Table S3). SNX1 protein was detected only in co-cultured BEC (Fig. 6b), while SNX6-positive structures showed a different trend than the VPS35-positive ones (Fig. 6e). Our data points out that the differentiation factors and astrocytes influence the various types of retromer in a separate and not a general way. In the retromer complex, the core complex (VPS35-VPS26-VPS35) is essential for the cargo/receptor selection, while the interchangeable SNX-BAR subunit is responsible to direct the subcellular trafficking toward different destinations [17]. Thus, it is likely that the different sets of retromer subtypes direct retrograde receptors in different directions in co-cultured BEC. For instance, the SNX1-retromer promotes E-cadherin trafficking to the TGN, from where it will be recycled to the plasma membrane of epithelial cells [74]. Since astrocytes are known to enhance localisation of E-cadherin to cell borders during co-culture [22], we suggest that SNX1-retromer is also involved in this process at the BBB. Further investigation is needed to support this hypothesis and to revile if SNX1-retromer guides only the E-cadherin or also the vascular endothelial specific VE-cadherin. Our observations on the retromer can be particularly interesting for receptor-mediated transcytosis in the light of a recent finding where the retromer-transported mannose-6-phosphate receptor was described as a potential target for receptor-mediated

Changes in gene expression level of co-cultured brain endothelial cells (RT-qPCR)											
a	**Protein**	**Gene name**	**Syber green gene expression assay**	**$2^{-\Delta\Delta CT}$ fold change**	**SEM**	**Control ($2^{-\Delta CT}$)**	**SEM**	**Co-cultured BEC ($2^{-\Delta CT}$)**	**SEM**	***p* value**	**Significance**
Adaptins [Ref]											
Ubiquitous [20]	AP-1A (μ1A)	*AP1M1*	NM_001243917.1	0.0082	0.0002	0.0952	0.0014	0.0735	0.0011	< 0.0001	***
Epithelial-specific [20]	AP-1B (μ1B)	*AP1M2*	XM_013987439.1	NE	NE	NE	NE	NE	NE	NE	NE
Epithelial-specific [20]	AP-1B (μ1B)	*AP1M2* +	XM_013987439.1			0.0095	0.0002				
Ubiquitous [75]	AP-3A (μ3A)	*AP3M1*	NM_001243516.1	1.1594	0.0000	0.2026	0.0016	0.1839	0.0007	< 0.0001	***
Neuron-specific [75]	AP-3B (μ3B)	*AP3M2*	XM_005657653.2	0.8746	0.0000	0.0074	0.0001	0.0051	0.0001	< 0.0001	***
Retromer complex											
	VPS35	*VPS35*	XM_013992400.1	1.5874	0.9769	0.3353	0.0048	0.3764	0.0069	0.0011	**
	VPS26A	*VPS26A*	XM_001925999.6	0.9013	0.9697	1.0187	0.0108	0.9183	0.0263	0.0036	**
	VPS26B	*VPS26B*	XM_013979597.1	0.8847	0.9823	0.1054	0.0015	0.0932	0.0010	0.0003	***
			NM_001137634.1								
	SNX1	*SNX1*	NM_001285972.1	0.1273	0.9341	0.0018	0.0001	0.0002	0.0000	< 0.0001	***
	SNX2	*SNX2*	XM_013986699.1	1.1251	0.9846	0.3686	0.0026	0.3276	0.0045	0.0002	***
	SNX5	*SNX5*	XM_013985097.1	0.6127	0.9841	0.2570	0.0018	0.1575	0.0023	< 0.0001	***
	SNX6	*TRAF4*	XM_005656996	0.7286	0.9476	0.0020	0.0002	0.0015	0.0001	0.0057	**

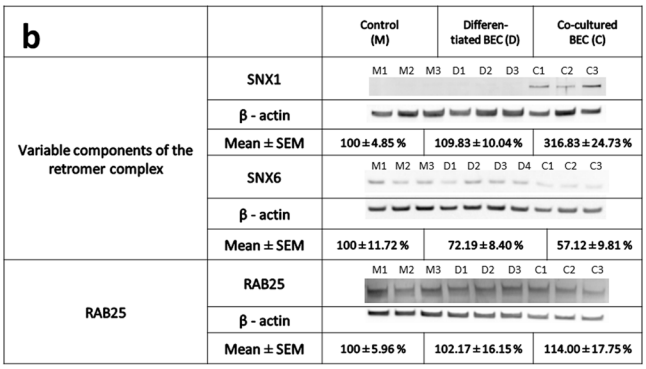

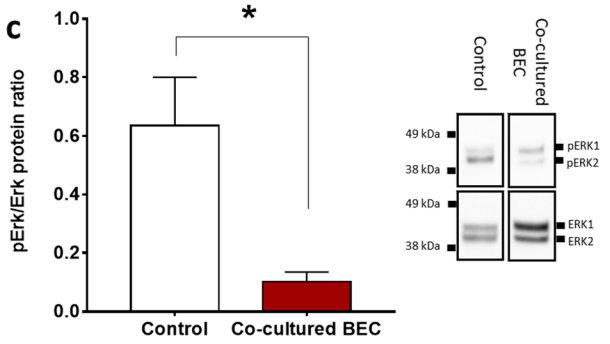

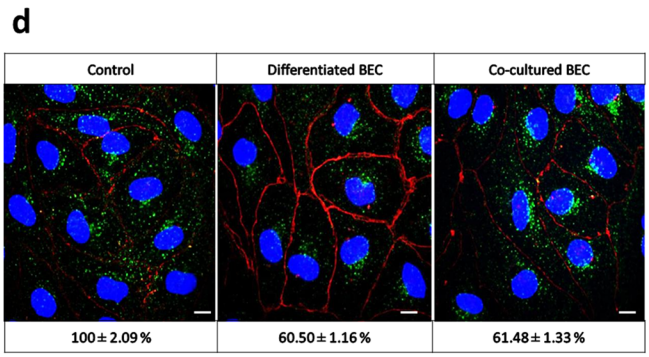

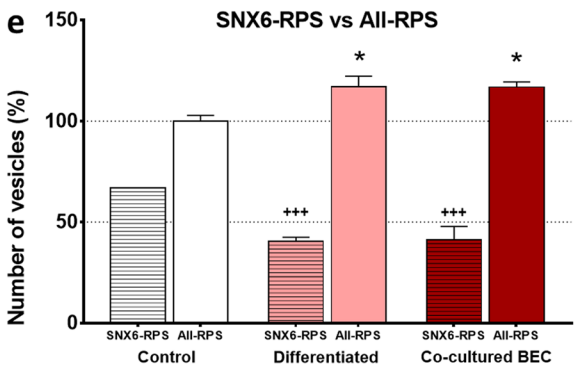

Fig. 6 Expression analysis of adaptor proteins in the BEC. **a** Changes in gene expression level of co-cultured BEC for selected trafficking-related genes. The table shows the fold change ($2^{-\Delta\Delta CT}$ values) in gene expression level of co-cultured BEC normalised to the gene expression level of the control ($2^{-\Delta\Delta CT}$) and measured by RT-qPCR method. 1 equals no change, < 1 = decrease, > 1 = increase in gene expression compared to control, $n = 9$. Statistics were carried out with unpaired *t* test with Welch's correction analysis. NE; not expressed. +; AP1M2 in porcine kidney homogenate. **b** Western blot for protein expression level of selected adaptor proteins in BEC in vitro. Intensity values of proteins were normalised to β-actin and then compared to the control (100%), $n = 12$. **c** Protein ratio of pERK1/2 and ERK1/2 by WB. Values expressed as mean ± SEM, $n = 12$. WB of one representative sample is shown in the right panel. Values were considered being statistically significant at $^{*}p < 0.05$. **d** Immunofluorescence for SNX6-RPS. Green staining indicates SNX6-RPS. The junctions of BEC were marked with antibody against tight junction protein, ZO1. For staining of nuclei Hoescht 32528 was used. Scale bar: 10 μm. Number of vesicles were normalised to the control (100%). **e** Change in the number of SNX6-positive retromer structures (SNX6-RPS) normalised to the total number of RPS (Vps35 positive) in control BEC (100%). All values are expressed as mean ± SEM, $n = 9$. Difference was analysed by one-way ANOVA followed by Tukey's post hoc test. Values were considered being statistically significant at $^{+++}p \leq 0.001$ compared to the SNX6-RPS control $^{*}p \leq 0.05$ compared to the Total-RPS control. ns; not significant

delivery of pharmaceutical antibodies in BEC [38]. Taken together, our present and previous [38] works confirm that the retromer and the retrograde receptors are present in BEC (Table S3). We have shown that the retromer is upregulated and different compositions of retromer subtypes are present in co-cultured BEC. These observations can highlight retrograde

receptors as efficient targets for drug transport toward the brain.

Trafficking among the structures of the endo-lysosomal system is guided by specific adaptor proteins such as adaptins [57]. The gene expression pattern of adaptins in BEC (Fig. S3) was similar to the adaptin copy number described in HeLa cells [56]. In polarised cells like epithelial cells and neurons, cell-specific isotopes of adaptors developed in evolution to ensure delivery of membrane components to the appropriate plasma membrane domain [57]. Since our current understanding of trafficking in BEC is mainly based on assumptions from studies of other polarised cells, we have investigated the expression of adaptin isoforms. In addition to the ubiquitously-expressed AP1-μ1A, polarised epithelial cells express the AP1-μ1B variant, which supports delivery of proteins, including β-catenin and TfR, to the basolateral domain [20]. Interestingly, the gene of AP1-μ1B (*AP1M2*) was not expressed in porcine BEC (Fig. 6a and Table S3) indicating that transport of receptor to the basal and lateral membrane in BEC needs sorting machinery different from that of epithelial cells. In order to further support the cell-specific expression of *AP1M2*, future studies should include BEC also from other species. Furthermore, we found that the previously known as neuron-specific gene of AP3-μ3B (*AP3M2*) [75] is expressed in BEC (Fig. 6a and Table S3). AP3-3μB is known to be responsible for synaptic vesicle formation [75]. Its role in BEC has not been described yet. Although contamination by neurons cannot be completely excluded, it is highly unlikely, as only cells expressing P-glycoprotein (like BEC) will survive the treatment with puromycin [69] during our BEC purification [76]. Our finding on distinctively expressed adaptor proteins in receptor trafficking might be useful to verify brain endothelial-specific transport machinery also in the currently developed human BBB models from induced pluripotent stem cells [77, 78]. Distinctive expression of *AP1M1* and *AP3M2* indicates for the first time that polarised trafficking in BEC differs from that of epithelia and therefore needs to be specifically examined.

For our investigation, we used porcine BEC, since their morphology and physiology are more similar to the human than rodent BEC [79]. Therefore, porcine BEC are highly suitable for the development of drug delivery strategies to future human applications. We investigated the effects of astrocytes and differentiation factors on the endo-lysosomal system of BEC. To reveal the effect of differentiation factors separately, we compared co-cultured BEC with monoculture of differentiated BEC. The differentiation mixture alone did not have such an influence on the vesicular system of BEC as it did in the presence of astrocytes. These results underline the importance of using co-culture models in in vitro studies where the vesicular system of BEC is in focus, such as receptor trafficking and drug delivery. We used cross-species co-culture model, since combination of porcine and rat astrocyte is one of the most widespread and accepted setup for in vitro BBB models based on primary cells [3]. A recent study has compared rat versus porcine astrocytes in co-culture with porcine BEC and no differences in BEC's barrier properties were reported [36], although effects on the transcellular or vesicular transport properties between these two models cannot be excluded. It should be analysed further in upcoming studies. Furthermore, it will be interesting to include pericytes in co-culture systems in follow-up studies, as these have been demonstrated to be involved in regulating transcytosis [80]. Particularly, peryicytes mediated downregulation of MFSD2A has been elegantly demonstrated to increase BEC transcytosis, as MFSD2A dramatically inhibits vesicular transcytosis across the BBB [81].

In conclusion, our study is the first to investigate the effects of astrocytes on the endo-lysosomal system in BEC by classifying the vesicles and transport routes with specific markers and adaptor proteins. We show that the expression of specific adaptor proteins in BEC differs in subtle ways from that of polarised epithelial cells. Data from our study may help improving to design strategies to traverse the BBB more intelligently.

Acknowledgements Niels M. Kristiansen, Annemette B. Marnow, Mitra Shamsali, Anders Heuck, and Tibor Salzer are thanked for their expert technical assistance. Matthias Rommeswinkel, applicant specialist at Olympus Soft Imaging Solutions GmbH, is acknowledged for his technical support in Scan^R Image analysis software. We thank N. Joan Abbott for critical reading of the manuscript.

Funding Information The work was supported by the Research Initiative on Brain Barriers and Drug Delivery funded by the Lundbeck foundation (Grant no. 2013-14113). KLH was supported by a grant from the Danish National Research Foundation (DNRF) (PUMPKIN DNRF85). The funders had no role in study design, data collection and interpretation, or the decision to submit the work for publication.

Compliance with Ethical Standards

Ethical Approval All applicable international, national, and/or institutional guidelines for the care and use of animals were followed. All animals were sacrificed following Danish legislation from the Danish Ministry of Environment and Food on slaughtering of animals (BEK no. 135 of 14/02/2014, European legislation identifier/eli/lta/2014/135). Rats were euthanized according to Danish legislation on animal experimentation (BEK number 12 of 07/01/2016, European legislation identifier/eli/lta/2016/12) and to the international guidelines on the ethical use of animals (European Communities Council Directive of 24 November 1986; 86/609/EEC). The ARRIVE guidelines have been followed.

Conflict of Interests The authors declare no conflict of interest.

References

1. Cecchelli R, Berezowski V, Lundquist S, Culot M, Renftel M, Dehouck MP, Fenart L (2007) Modelling of the blood-brain barrier

in drug discovery and development. Nat Rev Drug Discov 6(8): 650–661. https://doi.org/10.1038/nrd2368
2. Toth A, Veszelka S, Nakagawa S, Niwa M, Deli MA (2011) Patented in vitro blood-brain barrier models in CNS drug discovery. Recent Pat CNS Drug Discov 6(2):107–118
3. Helms HC, Abbott NJ, Burek M, Cecchelli R, Couraud PO, Deli MA, Forster C, Galla HJ et al (2016) In vitro models of the blood-brain barrier: an overview of commonly used brain endothelial cell culture models and guidelines for their use. J Cereb Blood Flow Metab 36(5):862–890. https://doi.org/10.1177/0271678X16630991
4. Salameh TS, Banks WA (2014) Delivery of therapeutic peptides and proteins to the CNS. Adv Pharmacol 71:277–299. https://doi.org/10.1016/bs.apha.2014.06.004
5. Herve F, Ghinea N, Scherrmann JM (2008) CNS delivery via adsorptive transcytosis. AAPS J 10(3):455–472. https://doi.org/10.1208/s12248-008-9055-2
6. Freskgard PO, Urich E (2017) Antibody therapies in CNS diseases. Neuropharmacology 120:38–55. https://doi.org/10.1016/j.neuropharm.2016.03.014
7. Preston JE, Joan Abbott N, Begley DJ (2014) Transcytosis of macromolecules at the blood-brain barrier. Adv Pharmacol 71:147–163. https://doi.org/10.1016/bs.apha.2014.06.001
8. Villasenor R, Kalaidzidis Y, Zerial M (2016) Signal processing by the endosomal system. Curr Opin Cell Biol 39:53–60. https://doi.org/10.1016/j.ceb.2016.02.002
9. Palfy M, Remenyi A, Korcsmaros T (2012) Endosomal crosstalk: meeting points for signaling pathways. Trends Cell Biol 22(9):447–456. https://doi.org/10.1016/j.tcb.2012.06.004
10. Stoops EH, Caplan MJ (2014) Trafficking to the apical and basolateral membranes in polarized epithelial cells. J Am Soc Nephrol: JASN 25(7):1375–1386. https://doi.org/10.1681/ASN.2013080883
11. Huotari J, Helenius A (2011) Endosome maturation. EMBO J 30(17):3481–3500. https://doi.org/10.1038/emboj.2011.286
12. Lajoie JM, Shusta EV (2015) Targeting receptor-mediated transport for delivery of biologics across the blood-brain barrier. Annu Rev Pharmacol Toxicol 55:613–631. https://doi.org/10.1146/annurev-pharmtox-010814-124852
13. Dempsey GP, Bullivant S, Watkins WB (1973) Endothelial cell membranes: polarity of particles as seen by freeze-fracturing. Science 179(4069):190–192
14. Hellinger E, Veszelka S, Toth AE, Walter F, Kittel A, Bakk ML, Tihanyi K, Hada V et al (2012) Comparison of brain capillary endothelial cell-based and epithelial (MDCK-MDR1, Caco-2, and VB-Caco-2) cell-based surrogate blood-brain barrier penetration models. Eur J Pharm Biopharm 82(2):340–351. https://doi.org/10.1016/j.ejpb.2012.07.020
15. Mayor S, Presley JF, Maxfield FR (1993) Sorting of membrane components from endosomes and subsequent recycling to the cell surface occurs by a bulk flow process. J Cell Biol 121(6):1257–1269
16. Maxfield FR, McGraw TE (2004) Endocytic recycling. Nat Rev Mol Cell Biol 5(2):121–132. https://doi.org/10.1038/nrm1315
17. Klinger SC, Siupka P, Nielsen MS (2015) Retromer-mediated trafficking of transmembrane receptors and transporters. Membranes (Basel) 5(3):288–306. https://doi.org/10.3390/membranes5030288
18. Sollner T, Whiteheart SW, Brunner M, Erdjument-Bromage H, Geromanos S, Tempst P, Rothman JE (1993) SNAP receptors implicated in vesicle targeting and fusion. Nature 362(6418):318–324. https://doi.org/10.1038/362318a0
19. Seaman MN, McCaffery JM, Emr SD (1998) A membrane coat complex essential for endosome-to-Golgi retrograde transport in yeast. J Cell Biol 142(3):665–681
20. Folsch H, Ohno H, Bonifacino JS, Mellman I (1999) A novel clathrin adaptor complex mediates basolateral targeting in polarized epithelial cells. Cell 99(2):189–198
21. Alvarez JI, Katayama T, Prat A (2013) Glial influence on the blood brain barrier. Glia 61(12):1939–1958. https://doi.org/10.1002/glia.22575
22. Rubin LL, Hall DE, Porter S, Barbu K, Cannon C, Horner HC, Janatpour M, Liaw CW et al (1991) A cell culture model of the blood-brain barrier. J Cell Biol 115(6):1725–1735
23. Hayashi Y, Nomura M, Yamagishi S, Harada S, Yamashita J, Yamamoto H (1997) Induction of various blood-brain barrier properties in non-neural endothelial cells by close apposition to co-cultured astrocytes. Glia 19(1):13–26
24. Sobue K, Yamamoto N, Yoneda K, Hodgson ME, Yamashiro K, Tsuruoka N, Tsuda T, Katsuya H et al (1999) Induction of blood-brain barrier properties in immortalized bovine brain endothelial cells by astrocytic factors. Neurosci Res 35(2):155–164
25. Haseloff RF, Blasig IE, Bauer HC, Bauer H (2005) In search of the astrocytic factor(s) modulating blood-brain barrier functions in brain capillary endothelial cells in vitro. Cell Mol Neurobiol 25(1):25–39
26. Worzfeld T, Schwaninger M (2016) Apicobasal polarity of brain endothelial cells. J. Cereb Blood Flow Metab 36(2):340–362. https://doi.org/10.1177/0271678X15608644
27. Prat A, Biernacki K, Wosik K, Antel JP (2001) Glial cell influence on the human blood-brain barrier. Glia 36(2):145–155. https://doi.org/10.1002/Glia.1104
28. Ezan P, Andre P, Cisternino S, Saubamea B, Boulay AC, Doutremer S, Thomas MA, Quenech'du N et al (2012) Deletion of astroglial connexins weakens the blood-brain barrier. J Cereb Blood Flow Metab 32(8):1457–1467. https://doi.org/10.1038/jcbfm.2012.45
29. Dehouck MP, Meresse S, Delorme P, Fruchart JC, Cecchelli R (1990) An easier, reproducible, and mass-production method to study the blood-brain barrier in vitro. J Neurochem 54(5):1798–1801
30. Hoheisel D, Nitz T, Franke H, Wegener J, Hakvoort A, Tilling T, Galla HJ (1998) Hydrocortisone reinforces the blood-brain barrier properties in a serum free cell culture system. Biochem Biophys Res Commun 244(1):312–316. https://doi.org/10.1006/bbrc.1997.8051
31. Patabendige A, Abbott NJ (2014) Primary porcine brain microvessel endothelial cell isolation and culture. Curr Protoc Neurosci 69(3.27):21–17. https://doi.org/10.1002/0471142301.ns0327s69
32. Igarashi Y, Utsumi H, Chiba H, Yamada-Sasamori Y, Tobioka H, Kamimura Y, Furuuchi K, Kokai Y et al (1999) Glial cell line-derived neurotrophic factor induces barrier function of endothelial cells forming the blood-brain barrier. Biochem Biophys Res Commun 261(1):108–112. https://doi.org/10.1006/bbrc.1999.0992
33. Abbott NJ, Ronnback L, Hansson E (2006) Astrocyte-endothelial interactions at the blood-brain barrier. Nat Rev Neurosci 7(1):41–53. https://doi.org/10.1038/nrn1824
34. Neuhaus W, Gaiser F, Mahringer A, Franz J, Riethmuller C, Forster C (2014) The pivotal role of astrocytes in an in vitro stroke model of the blood-brain barrier. Front Cell Neurosci 8:352. https://doi.org/10.3389/fncel.2014.00352
35. Nielsen SSE, Siupka P, Georgian A, Preston JE, Toth AE, Yusof SR, Abbott NJ, Nielsen MS (2017) Improved method for the establishment of an in vitro blood-brain barrier model based on porcine brain endothelial cellsJ Vis Exp 127(127). doi:https://doi.org/10.3791/56277
36. Thomsen LB, Burkhart A, Moos T (2015) A triple culture model of the blood-brain barrier using porcine brain endothelial cells, astrocytes and Pericytes. PLoS One 10(8):e0134765. https://doi.org/10.1371/journal.pone.0134765

37. Patabendige A, Skinner RA, Morgan L, Abbott NJ (2013) A detailed method for preparation of a functional and flexible blood-brain barrier model using porcine brain endothelial cells. Brain Res 1521:16–30. https://doi.org/10.1016/j.brainres.2013.04.006
38. Siupka P, Hersom MN, Lykke-Hartmann K, Johnsen KB, Thomsen LB, Andresen TL, Moos T, Abbott NJ et al (2017) Bidirectional apical-basal traffic of the cation-independent mannose-6-phosphate receptor in brain endothelial cells. J Cereb Blood Flow Metab 37(7):2598–2613. https://doi.org/10.1177/0271678X17700665
39. Jensen NA, Gerth K, Grotjohann T, Kapp D, Keck M, Niehaus K (2009) Establishment of a high content assay for the identification and characterisation of bioactivities in crude bacterial extracts that interfere with the eukaryotic cell cycle. J Biotechnol 140(1–2):124–134. https://doi.org/10.1016/j.jbiotec.2008.12.002
40. Matrone C, Dzamko N, Madsen P, Nyegaard M, Pohlmann R, Sondergaard RV, Lassen LB, Andresen TL et al (2016) Mannose 6-phosphate receptor is reduced in synuclein overexpressing models of Parkinsons disease. PLoS One 11(8):e0160501. https://doi.org/10.1371/journal.pone.0160501
41. Kim D, Pertea G, Trapnell C, Pimentel H, Kelley R, Salzberg SL (2013) TopHat2: accurate alignment of transcriptomes in the presence of insertions, deletions and gene fusions. Genome Biol 14(4):R36. https://doi.org/10.1186/gb-2013-14-4-r36
42. Anders S, Pyl PT, Huber W (2015) HTSeq—a Python framework to work with high-throughput sequencing data. Bioinformatics 31(2):166–169. https://doi.org/10.1093/bioinformatics/btu638
43. Dillies MA, Rau A, Aubert J, Hennequet-Antier C, Jeanmougin M, Servant N, Keime C, Marot G et al (2013) A comprehensive evaluation of normalization methods for Illumina high-throughput RNA sequencing data analysis. Brief Bioinform 14(6):671–683. https://doi.org/10.1093/bib/bbs046
44. Quackenbush J (2002) Microarray data normalization and transformation. Nat Genet 32(Suppl):496–501. https://doi.org/10.1038/ng1032
45. Subramanian A, Tamayo P, Mootha VK, Mukherjee S, Ebert BL, Gillette MA, Paulovich A, Pomeroy SL et al (2005) Gene set enrichment analysis: a knowledge-based approach for interpreting genome-wide expression profiles. Proc Natl Acad Sci U S A 102(43):15545–15550. https://doi.org/10.1073/pnas.0506580102
46. Kanehisa M, Furumichi M, Tanabe M, Sato Y, Morishima K (2017) KEGG: new perspectives on genomes, pathways, diseases and drugs. Nucleic Acids Res 45(D1):D353–D361. https://doi.org/10.1093/nar/gkw1092
47. Andersen CL, Jensen JL, Orntoft TF (2004) Normalization of real-time quantitative reverse transcription-PCR data: a model-based variance estimation approach to identify genes suited for normalization, applied to bladder and colon cancer data sets. Cancer Res 64(15):5245–5250. https://doi.org/10.1158/0008-5472.CAN-04-0496
48. Schmittgen TD, Livak KJ (2008) Analyzing real-time PCR data by the comparative C(T) method. Nat Protoc 3(6):1101–1108
49. Patki V, Virbasius J, Lane WS, Toh BH, Shpetner HS, Corvera S (1997) Identification of an early endosomal protein regulated by phosphatidylinositol 3-kinase. Proc Natl Acad Sci U S A 94(14):7326–7330
50. Dautry-Varsat A, Ciechanover A, Lodish HF (1983) pH and the recycling of transferrin during receptor-mediated endocytosis. Proc Natl Acad Sci U S A 80(8):2258–2262
51. Chavrier P, Parton RG, Hauri HP, Simons K, Zerial M (1990) Localization of low molecular weight GTP binding proteins to exocytic and endocytic compartments. Cell 62(2):317–329
52. Lewis V, Green SA, Marsh M, Vihko P, Helenius A, Mellman I (1985) Glycoproteins of the lysosomal membrane. J Cell Biol 100(6):1839–1847
53. Li X, Rydzewski N, Hider A, Zhang X, Yang J, Wang W, Gao Q, Cheng X et al (2016) A molecular mechanism to regulate lysosome motility for lysosome positioning and tubulation. Nat Cell Biol 18(4):404–417. https://doi.org/10.1038/ncb3324
54. De Bock M, Van Haver V, Vandenbroucke RE, Decrock E, Wang N, Leybaert L (2016) Into rather unexplored terrain-transcellular transport across the blood-brain barrier. Glia 64(7):1097–1123. https://doi.org/10.1002/glia.22960
55. Cullen PJ, Korswagen HC (2011) Sorting nexins provide diversity for retromer-dependent trafficking events. Nat Cell Biol 14(1):29–37. https://doi.org/10.1038/ncb2374
56. Hirst J, Irving C, Borner GH (2013) Adaptor protein complexes AP-4 and AP-5: new players in endosomal trafficking and progressive spastic paraplegia. Traffic 14(2):153–164. https://doi.org/10.1111/tra.12028
57. Ohno H (2006) Clathrin-associated adaptor protein complexes. J Cell Sci 119(Pt 18):3719–3721. https://doi.org/10.1242/jcs.03085
58. Skinner RA, Gibson RM, Rothwell NJ, Pinteaux E, Penny JI (2009) Transport of interleukin-1 across cerebromicrovascular endothelial cells. Br J Pharmacol 156(7):1115–1123. https://doi.org/10.1111/j.1476-5381.2008.00129.x
59. Candela P, Gosselet F, Saint-Pol J, Sevin E, Boucau MC, Boulanger E, Cecchelli R, Fenart L (2010) Apical-to-basolateral transport of amyloid-beta peptides through blood-brain barrier cells is mediated by the receptor for advanced glycation end-products and is restricted by P-glycoprotein. J Alzheimer's Dis: JAD 22(3):849–859. https://doi.org/10.3233/JAD-2010-100462
60. Kaur C, Sivakumar V, Zhang Y, Ling EA (2006) Hypoxia-induced astrocytic reaction and increased vascular permeability in the rat cerebellum. Glia 54(8):826–839. https://doi.org/10.1002/glia.20420
61. Andras IE, Leda A, Contreras MG, Bertrand L, Park M, Skowronska M, Toborek M (2017) Extracellular vesicles of the blood-brain barrier: role in the HIV-1 associated amyloid beta pathology. Mol Cell Neurosci 79:12–22. https://doi.org/10.1016/j.mcn.2016.12.006
62. Wolburg H, Lippoldt A (2002) Tight junctions of the blood-brain barrier: development, composition and regulation. Vasc Pharmacol 38(6):323–337
63. Nielsen E, Severin F, Backer JM, Hyman AA, Zerial M (1999) Rab5 regulates motility of early endosomes on microtubules. Nat Cell Biol 1(6):376–382. https://doi.org/10.1038/14075
64. Thompson A, Nessler R, Wisco D, Anderson E, Winckler B, Sheff D (2007) Recycling endosomes of polarized epithelial cells actively sort apical and basolateral cargos into separate subdomains. Mol Biol Cell 18(7):2687–2697. https://doi.org/10.1091/mbc.E05-09-0873
65. Luzio JP, Pryor PR, Bright NA (2007) Lysosomes: fusion and function. Nat Rev Mol Cell Biol 8(8):622–632. https://doi.org/10.1038/nrm2217
66. Thauerer B, Voegele P, Hermann-Kleiter N, Thuille N, de Araujo ME, Offterdinger M, Baier G, Huber LA et al (2014) LAMTOR2-mediated modulation of NGF/MAPK activation kinetics during differentiation of PC12 cells. PLoS One 9(4):e95863. https://doi.org/10.1371/journal.pone.0095863
67. Miller F, Fenart L, Landry V, Coisne C, Cecchelli R, Dehouck MP, Buee-Scherrer V (2005) The MAP kinase pathway mediates transcytosis induced by TNF-alpha in an in vitro blood-brain barrier model. Eur J Neurosci 22(4):835–844. https://doi.org/10.1111/j.1460-9568.2005.04273.x
68. Larner A, B Z (2018) Screening for obstructive sleep apnoea using the STOPBANG questionnaire. Clin Med 18(1):108–109. https://doi.org/10.7861/clinmedicine.18-1-108a
69. Perriere N, Demeuse P, Garcia E, Regina A, Debray M, Andreux JP, Couvreur P, Scherrmann JM et al (2005) Puromycin-based purification of rat brain capillary endothelial cell cultures. Effect on the

expression of blood-brain barrier-specific properties. J Neurochem 93(2):279–289. https://doi.org/10.1111/j.1471-4159.2004.03020.x

70. Tzaban S, Massol RH, Yen E, Hamman W, Frank SR, Lapierre LA, Hansen SH, Goldenring JR et al (2009) The recycling and transcytotic pathways for IgG transport by FcRn are distinct and display an inherent polarity. J Cell Biol 185(4):673–684. https://doi.org/10.1083/jcb.200809122
71. Casanova JE, Wang X, Kumar R, Bhartur SG, Navarre J, Woodrum JE, Altschuler Y, Ray GS et al (1999) Association of Rab25 and Rab11a with the apical recycling system of polarized Madin-Darby canine kidney cells. Mol Biol Cell 10(1):47–61
72. Mellado M, Cuartero Y, Brugada R, Verges M (2014) Subcellular localisation of retromer in post-endocytic pathways of polarised Madin-Darby canine kidney cells. Biol Cell 106(11):377–393. https://doi.org/10.1111/boc.201400011
73. Bundgaard M (1987) Tubular invaginations in cerebral endothelium and their relation to smooth-surfaced cisternae in hagfish (*Myxine glutinosa*). Cell Tissue Res 249(2):359–365. https://doi.org/10.1007/bf00215520
74. Bryant DM, Kerr MC, Hammond LA, Joseph SR, Mostov KE, Teasdale RD, Stow JL (2007) EGF induces macropinocytosis and SNX1-modulated recycling of E-cadherin. J Cell Sci 120(Pt 10):1818–1828. https://doi.org/10.1242/jcs.000653
75. Faundez V, Horng JT, Kelly RB (1998) A function for the AP3 coat complex in synaptic vesicle formation from endosomes. Cell 93(3):423–432
76. Nielsen SS, Siupka P, Georgian A, Preston JE, Tóth AE, Yusof SR, Abbott NJ, Nielsen MS (2017) Improved method for the establishment of an in vitro blood-brain barrier model based on porcine brain endothelial cells. J Vis Exp e56277. doi:https://doi.org/10.3791/56277
77. Stebbins MJ, Wilson HK, Canfield SG, Qian T, Palecek SP, Shusta EV (2016) Differentiation and characterization of human pluripotent stem cell-derived brain microvascular endothelial cells. Methods 101:93–102. https://doi.org/10.1016/j.ymeth.2015.10.016
78. Appelt-Menzel A, Cubukova A, Gunther K, Edenhofer F, Piontek J, Krause G, Stuber T, Walles H et al (2017) Establishment of a human blood-brain barrier co-culture model mimicking the neurovascular unit using induced pluri- and multipotent stem cells. Stem cell Rep 8(4):894–906. https://doi.org/10.1016/j.stemcr.2017.02.021
79. Kubo Y, Ohtsuki S, Uchida Y, Terasaki T (2015) Quantitative determination of luminal and abluminal membrane distributions of transporters in porcine brain capillaries by plasma membrane fractionation and quantitative targeted proteomics. J Pharm Sci 104(9):3060–3068. https://doi.org/10.1002/jps.24398
80. Armulik A, Genove G, Mae M, Nisancioglu MH, Wallgard E, Niaudet C, He L, Norlin J et al (2010) Pericytes regulate the blood-brain barrier. Nature 468(7323):557–561. https://doi.org/10.1038/nature09522
81. Ben-Zvi A, Lacoste B, Kur E, Andreone BJ, Mayshar Y, Yan H, Gu C (2014) Mfsd2a is critical for the formation and function of the blood-brain barrier. Nature 509(7501):507–511. https://doi.org/10.1038/nature13324